# Biomimetic silicification of 3D polyamine-rich scaffolds assembled by direct ink writing

Mingjie Xu,[a] Gregory M. Gratson,[b] Eric B. Duoss,[b] Robert F. Shepherd[b] and Jennifer A. Lewis*[ab]

*Received 6th December 2005, Accepted 23rd January 2006*
*First published as an Advance Article on the web 6th February 2006*
**DOI: 10.1039/b517278k**

**We report a method for creating synthetic diatom frustules *via* the biomimetic silicification of polyamine-rich scaffolds assembled by direct ink writing (DIW) [G. M. Gratson, M. Xu and J. A. Lewis, *Nature*, 2004, 428, 386, ref. 1]. A concentrated polyamine-rich ink is robotically deposited in a complex 3D pattern that mimics the shape of naturally occurring diatom frustules, *Triceratium favus* Ehrenberg (triangular-shaped) and *Arachnoidiscus ehrenbergii* (web-shaped). Upon exposing these scaffolds to silicic acid under ambient conditions, silica formation occurs in a shape-preserving fashion. Our method yields 3D inorganic–organic hybrids structures that may find potential application as templates for photonic materials, novel membranes, or catalyst supports.**

## Introduction

Diatoms are unicellular algae best known for their ability to create complex silica cell walls under ambient physiological conditions. Their three-dimensional (3D) hierarchical patterns are both species-specific and genetically determined[2,3]. Organic macromolecules, such as silaffin peptides[4,5] and polyamines,[2] that regulate biosilica morphogenesis have been identified. Such species have been separated from diatoms and shown to catalyze silica formation under physiological conditions. Synthetic amino acids[6], peptides[7,8] and polyamines[9,10] are also known to catalyze the hydrolysis and condensation of silica precursors under ambient conditions. Building on these recent discoveries, several biomimetic approaches for creating ordered silica patterns from synthetic peptides, such as block polypeptide templating[8] and holographic patterning,[7] have been introduced. To date, however, none are able to replicate the level of structural sophistication exhibited by naturally occurring diatoms.

We recently demonstrated that 3D micro-periodic scaffolds of arbitrary shape can be assembled by direct writing of concentrated polyelectrolyte inks.[1,11] These scaffolds possess characteristic feature sizes that are nearly two orders of magnitude smaller than those attained by other multilayer ink printing techniques.[1,12] Here, we describe a new approach for templating 3D hybrid silica–organic structures that combines DIW with biomimetic silicification. Central to our approach is the creation of a synthetic polyamine-rich ink capable of being both patterned by DIW and subsequently mineralized *via* the hydrolysis and condensation of silica precursors. After silicification, their silica content and structure is investigated by thermogravimetric analysis (TGA), scanning electron microscopy and Auger electron spectroscopy. We found that preheating the scaffolds to promote amide bond formation followed by silicification provides a shape-preserving route for mineralizing these polyamine-rich scaffolds.

[a]*Department of Chemical and Biomolecular Engineering, University of Illinois at Urbana–Champaign, Champaign, IL, USA 61801. E-mail: mxu1@uiuc.edu; Tel: 1 217 244-4527*
[b]*Department of Material Science and Engineering, University of Illinois at Urbana–Champaign, Champaign, IL, USA 61801. E-mail: jalewis@uiuc.edu; Fax: 1 217 333-2736; Tel: 1 217 244-4937*

## Experimental

### Materials system

Poly(allylamine hydrochloride) (PAH) is a cationic polyelectrolyte comprised of a linear backbone with one primary amine side chain per monomer unit. PAH ($M_w \sim 60\,000$) was supplied by Polysciences (Warrington, PA) as a powder. Poly(acrylic acid) (PAA) sodium salt is an anionic polyelectrolyte with a linear backbone comprised of one ionizable [COONa] group per monomer unit. PAA ($M_w \sim 1200$) was purchased from Aldrich (Milwaukee, WI) as a concentrated aqueous solution (45% by weight). The typical coagulation reservoir was prepared by mixing 2-propanol (IPA) (ACS grade, Fisher Scientific, Fair Lawn, NJ), ethyl alcohol (Absolute, Aaper Alcohol and Chemical Co., Shelbyville, KY) and deionized water in a volumetric ratio of 80 (IPA) : 9 (ethanol) : 11 (water). All chemicals were used as received.

### Polyamine-rich inks

Concentrated polyelectrolyte complexes with a 2 : 1 ratio of [$NH_x$] : [COONa] ratio are produced by mixing appropriate amounts of PAH ($M_w \sim 60\,000$), PAA ($M_w \sim 1200$) and water, such that the total polymer concentration is 50% by weight. Immediately after mixing, an opaque precipitate forms. Upon magnetically stirring the mixture for 24 h, this opaque phase disappears yielding a transparent, homogeneous polyelectrolyte-based ink suitable for direct writing.

### Three-dimensional scaffold fabrication

Three-dimensional (3D) polymer scaffolds with micron-sized features are assembled using a robotic deposition apparatus (ABL9000, Aerotech Inc., Pittsburgh, PA). These complex 3D structures are defined using a computer-aided, direct-write program (RoboCAD) that controls the 3-axis motion of the micropositioning stage. The ink delivery system is mounted onto a

moving *xyz* stage for agile printing onto a stationary substrate. The ink is housed in a syringe (barrel diameter = 4.6 mm, EFD Inc., East Providence, RI) and deposited through a pulled borosilicate glass nozzle (μ-Tip, World Precision Instruments, Inc., Sarasota, FL) under an applied pressure (800 Ultra dispensing system, EFD Inc.) to maintain a constant flow rate at a deposition speed of 40 μm $s^{-1}$.

3D polymer scaffolds are assembled by patterning an array of rod-like filaments in a layer-by-layer build sequence. The spacing between layers ($\Delta z$) is equivalent to the nozzle diameter ($D$ = 1 μm), such that the intersections between rods can survive subsequent drying and silicification procedures. For triangular-shaped scaffolds, the first layer is composed of an array of rod-like filaments confined within a triangular shape (base = 160 μm) with curved edges. Subsequent layers are deposited in a similar pattern except that it is rotated by 120° between each layer. Web-shaped structures are produced by sequential deposition of layers with alternating patterns of concentric rings and circular arrays of radially oriented rods ($t \sim 8$ min). The first layer consists of a series of equally spaced concentric circles with radius ranging from 10 μm to 90 μm moving from inner to outer radius. In the subsequent layer, an array of radially oriented rods is deposited between the inner and outer radii. The angular spacing between the rods is 12.41°, such that the arc length between adjacent rods varied from 0 to 20 μm moving from the inner to outer radius. The build time ($t$) varies with the structure size and road width (*e.g.*, $t \sim 5$ min for a six-layer, triangular-shaped structure comprised of a 160 μm base with a 6 μm road width). All structures are dried at ~22 °C and less than 35% relative humidity.

### Thick film fabrication

Thick polymer films (50 ± 10 μm) are used to quantify the extent of silica formation throughout a given film after the silicification process. The films are fabricated by spin-coating the polyamine-rich ink onto a 2 × 2 $cm^2$ glass slide at 3000 rpm for 30 s. An appropriate amount of IPA is placed on the film surface after spin-coating to simulate the coagulation that occurs when ink filaments are deposited into the deposition reservoir during DIW.

### Silicification of polyamine-rich scaffolds and films

Representative 3D polyamine-rich scaffolds and thick films are partially cross-linked by heating at a rate of 5 °C $min^{-1}$ to 80 °C in air (hold time = 3 h) followed by heating at 5 °C $min^{-1}$ to 180 °C (hold time = 3 h), then cooling to room temperature at −5 °C $min^{-1}$. Biomimetic silicification of both as-fabricated and preheated 3D scaffolds and thick films is carried out using a single or sequential immersion method under ambient conditions. In the first method, the 3D scaffolds are immersed in 3.5 ml of an aqueous phosphate buffered (pH 8, 15 mM) silicic acid (50 mM) solution for 48 h followed by thorough rinsing with deionizied water. In the second method, these scaffolds are first immersed in 3.5 ml of an aqueous silicic acid (pH 3, 50 mM) solution for 48 h, and then immersed into 3.5 ml phosphate buffer solution (pH 8, 30 mM) for 0.5 h followed by thorough rinsing with deionized water. Note, polymer thick films are silicified by the same methods, except that the solution amounts are doubled to ensure an excess of silica precursor species.

### Scaffold characterization

SEM images are obtained using a Hitachi S-4700 Scanning Electron Microscope (Hitachi Ltd., Tokyo, Japan). After fabrication and drying, structures are mounted and sputtered with gold/palladium for 20 s (Emitech K575 Sputter Coater, Emitech Ltd., Ashford Kent, UK) prior to imaging.

After silicification, the silica content of polymer thick films is determined by thermogravimetric analysis (TGA). These films are first dried at 100 °C for 2 h and 150 °C for 5 min to remove any residual water. The samples are then transferred to the TGA (Mettler Toledo TGA/SDTA851[e]) and heated from 25 °C to 1000 °C at 10 °C $min^{-1}$ in air.

Focused ion beam (FIB) milling (FEI dual-beam DB-235) is used to expose a vertical cross-section through the silicified scaffolds. The ion current employed for etching and cleaning in FIB were 3000 pA and 500 pA, respectively. Silicon and oxygen elemental line scans and mapping are carried out using Auger electron spectroscopy (PHI 660 scanning Auger microprobe).

## Results and discussion

Direct writing of concentrated polyelectrolyte inks enables the assembly of 3D micro-patterned structures that emulate the stunning shapes exhibited by naturally occurring diatom frustules (see Fig. 1). Specifically, we choose to mimic the diatoms, *Triceratium favus* Ehrenberg (triangular-shaped structure) and *Arachnoidiscus ehrenbergii* (web-shaped structure). As Fig. 1 reveals, these patterned structures emulate the natural frustules in both their overall dimensions (~100–200 μm in size) and finer-scale details. The ability to rapidly pattern these 3D scaffolds allows to produce arrays of individual structures side-by-side on a given substrate.

The biomimetic silicification of these 3D polyamine-rich scaffolds to produce synthetic diatom frustules must satisfy two important requirements. First, their intricately patterned features

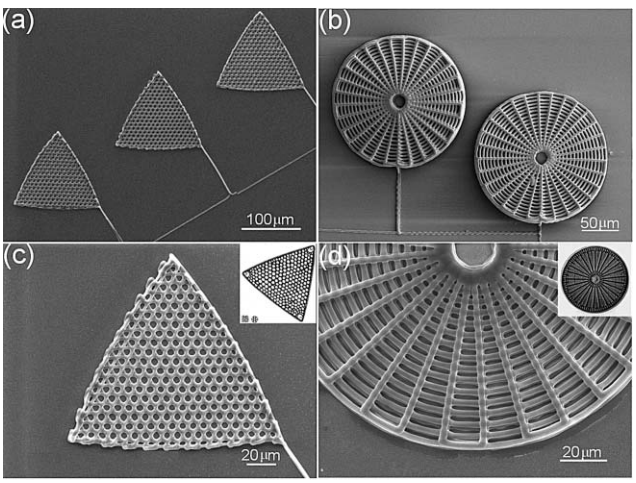


**Fig. 1** SEM images of (a) triangular- and (b) web-shaped polyamine-rich scaffolds assembled by direct ink writing, and corresponding higher magnification views of (c) triangular- and (d) web-shaped scaffolds. [Insets: Natural diatom species (c) *Triceratium favus* Ehrenberg and (d) *Arachnoidiscus ehrenbergii*.]

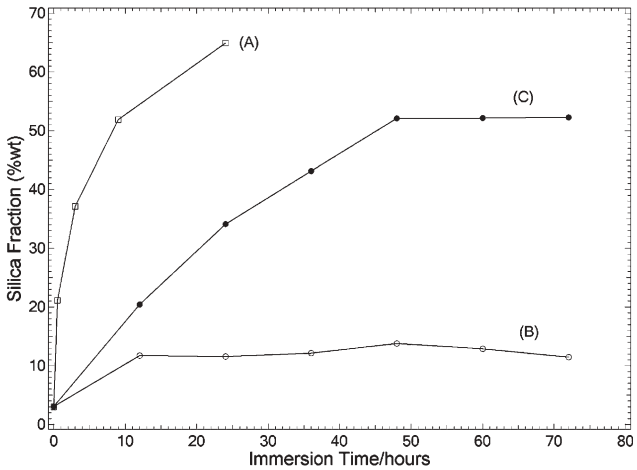


**Fig. 2** Silica content (wt% of total mass) of polymer films (thickness 50 μm) as a function of varying silicification methods: (A) as-cast film, single immersion, (B) partially cross-linked film, single immersion, and (C) partially cross-linked film, sequential immersion.

must be preserved during the templating process. This poses a significant challenge, since the structural integrity of the polyelectrolyte scaffolds depends strongly on pH and ionic strength.[11] Second, silica condensation must occur throughout the scaffolds to yield the desired inorganic–organic hybrids. We explore the silicification of polyamine-rich scaffolds and thick films using both a single and sequential immersion method under ambient conditions. The first method is similar to prior *in vitro* experiments, in which silica nanoparticles formed rapidly *via* an amine-mediated mechanism,[5,9,13] upon exposing a polyamine solution to a phosphate-buffered, silicic acid solution.

To quantify the total silica yield from each silicification method, thermogravimetric analysis (TGA) is carried out on corresponding polymer films subjected to same process conditions as the 3D scaffolds. A 2D architecture is adopted, because the low scaffold mass prohibits direct measurement using this technique. The TGA results shown in Fig. 2 reveal that silica condensation occurs to the greatest extent for the as-fabricated, polyamine-rich films. These films rapidly dissolve in the phosphate-buffered, silicic acid solution, promoting the formation of silica nanoparticle clusters. When the films are first heated to 180 °C to induce partial cross-linking between the PAH and PAA chains through amide bond formation[14] to enhance their structural integrity and then immersed in this same solution, they possess the lowest silica content (~11 wt%, Fig. 2(B)) observed. Alternatively, partially cross-linked films that undergo sequential immersion exhibit a nearly five-fold increase in their silica content (~52 wt%, Fig. 2 (C)) under identical immersion times (48 h). We attribute this dramatic increase in silica formation to the fact that during sequential immersion, the silica precursors are first allowed to diffuse through the film prior to being catalyzed by the addition of phosphate buffer, whereas in the single immersion method, precursor diffusion and silica formation occur simultaneously.

To explore the effects of silicification on the structure and composition of 3D polyamine-rich scaffolds, we exposed both as-patterned and partially cross-linked structures to the same conditions as their thick film analogs. The as-patterned scaffolds rapidly dissolved in solution yielding silica nanoparticle clusters (see Fig. 3a). However, as with the thick films, their structural integrity is enhanced by partial cross-linking at elevated temperature. These partially cross-linked scaffolds remain intact during either silicification process, *i.e.*, their overall shape as well as their fine features are preserved with high precision (see Fig. 3).

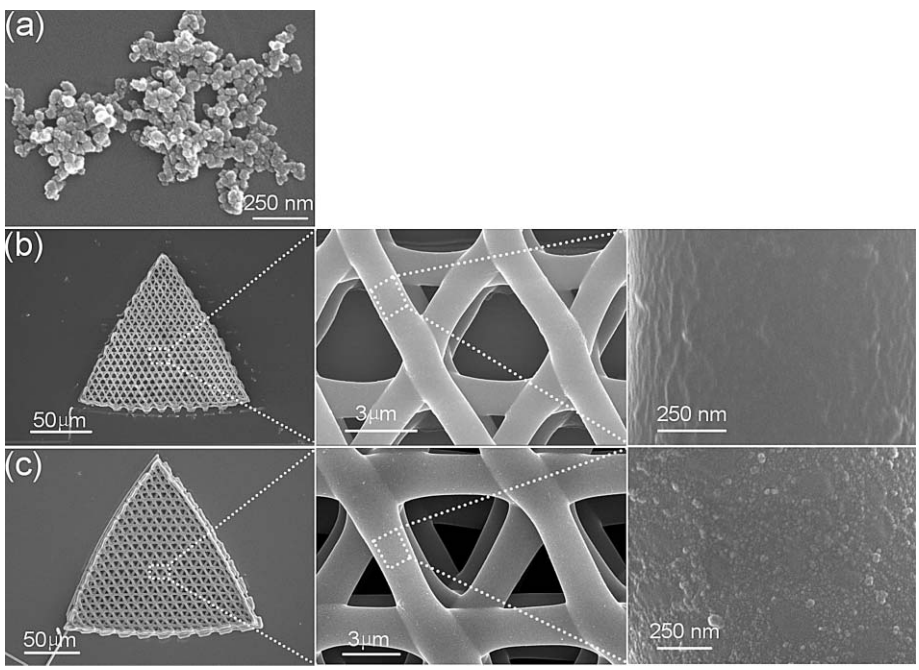


**Fig. 3** SEM images of 3D triangular-shaped, polyelectrolyte scaffolds after silicification: (a) as-patterned scaffold, single immersion (b) partially cross-linked scaffold, single immersion, and (c) partially cross-linked scaffold, sequential immersion. Corresponding higher magnification images of their structure are presented alongside those scaffolds whose shape was preserved during silicification.

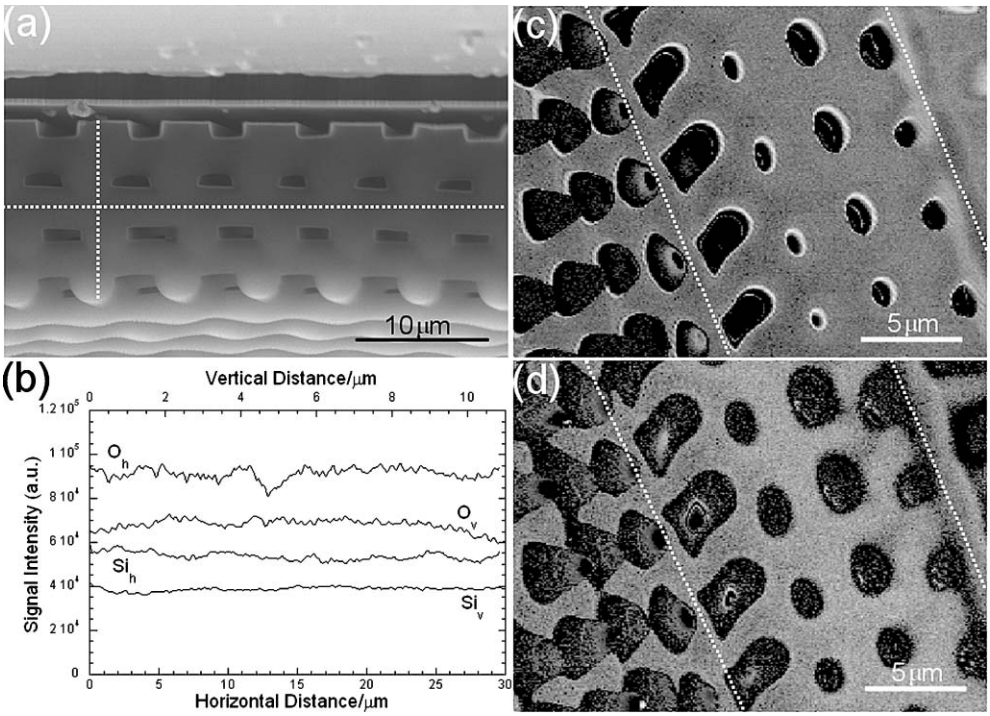


**Fig. 4** (a) SEM image of a focus ion beam (FIB) milled, cross-section of a partially cross-linked polyelectrolyte scaffold silicified by the sequential immersion method, (b) Auger line scans of silicon (Si) and oxygen (O) elements along vertical dashed line ($Si_v$ and $O_v$) and along horizontal dashed line ($Si_h$ and $O_h$), and (c) Si map and (d) O map of this structure.

However, partially cross-linked, 3D scaffolds silicified by the single immersion method exhibit little evidence of silica condensation on the scaffold surface (see Fig. 3b), whereas those silicified by the sequential immersion method possess a dense coating of silica nanoparticles on their surface (see Fig. 3c).

To determine whether partially cross-linked, 3D scaffolds subjected to the sequential immersion process are silicified throughout their structure, we use Auger electron spectroscopy (AES) to map the silicon and oxygen concentration across a FIB-milled, cross-section comprised of dense cylindrical filaments (see Fig. 4a). Horizontal and vertical line scans (Fig. 4b) and elemental mapping (Fig. 4c, d) indicate that silicon (Si) and oxygen (O) elements are distributed in a reasonably uniform fashion throughout the entire scaffold. Moreover, while partially cross-linked scaffolds maintain their structural integrity during either silicification method, only those that are immersed sequentially remain intact after the organic phase is removed from the hybrid structures by heating them to 1000 °C (see Fig. 5). Note, a two-fold decrease in their overall size is observed after heat treatment. This dimensional change is expected given their silica content (~52%) determined by TGA.

## Conclusions

We have created 3D synthetic diatom frustules by combining direct-write assembly of polyamine-rich inks with biomimetic silicification. Under the appropriate conditions, silica condensation occurs uniformly throughout the scaffolds leading to their enhanced thermal and mechanical stability. These silicified structures emulate natural diatoms in their degree of structural complexity and overall dimensions. As recently demonstrated for natural diatom frustules, we anticipate that these silicified structures can be readily converted to other materials, such as MgO[15] or titania[16] through a halide gas/solid displacement reaction. Other templating strategies, such as coating these structures

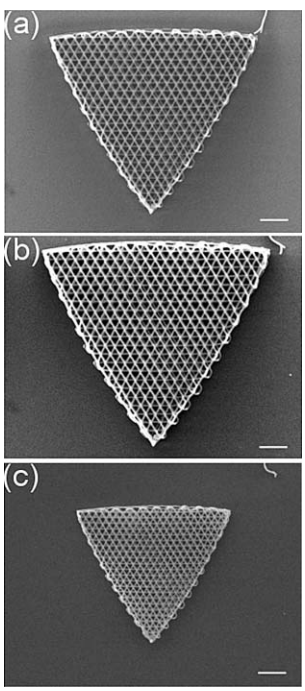


**Fig. 5** SEM images of triangular-shaped polyelectrolyte scaffolds showing their structural evolution: (a) as-patterned scaffold, (b) partially cross-linked scaffold after silicification by the sequential immersion method, and (c) silica scaffold after heat treatment at 1000 °C. [All scale bars 20 μm].

 

by silicon chemical vapor deposition,[17] may enable their application as photonic band gap materials. More generally, our ink design can be extended to incorporate natural or synthetic polypeptides that allow a broader range of biomineralization strategies to be pursued, which when coupled with our ability to pattern 3D structures of arbitrary shape and periodicity, may open up new avenues for soft-to-hard matter conversion under ambient conditions

## Acknowledgements

This material is based on work (direct ink writing) supported by the US Department of Energy, Division of Materials Sciences, under Award No. DEFG-02-91ER45439, through the Frederick Seitz Materials Research Laboratory at the University of Illinois at Urbana–Champaign, the US Army Research Laboratory and the US Army Research Office (multifunctional ceramic composites) under Award No. DAAD19-03-1-0227, and the Air Force Office of Scientific Research (biomineralization) under Award No. FA9550-05-1-0092 (Subaward No. E-18-C45-G1). This work was carried out in part in the Center for Microanalysis of Materials, University of Illinois, which is partially supported by the US Department of Energy under grant DEFG02-91-ER45439. We thank Nancy Finnegan and Jian-Guo Wen for their experimental assistance, and Ken Sandhage for useful discussions.

## References

1 G. M. Gratson, M. Xu and J. A. Lewis, *Nature*, 2004, **428**, 386.
2 N. Kroger, R. Deutzmann, C. Bergsdorf and M. Sumper, *Proc. Natl. Acad. Sci. U. S. A.*, 2000, **97**, 14133–14138.
3 M. Hildebrand, B. E. Volcani, W. Gassmann and J. I. Schroeder, *Nature*, 1997, **385**, 688–689.
4 N. Kroger, R. Deutzmann and M. Sumper, *Science*, 1999, **286**, 1129–1132.
5 N. Kroger, S. Lorenz, E. Brunner and M. Sumper, *Science*, 2002, **298**, 584–586.
6 D. Belton, G. Paine, S. V. Patwardhan and C. C. Perry, *J. Mater. Chem.*, 2004, **14**, 2231–2241.
7 L. L. Brett, R. R. Naik, D. J. Pikas, S. M. Kirkpatrlck, D. W. Tomlin, P. W. Whitlock, S. J. Clarsen and M. O. Stone, *Nature*, 2001, **413**, 291–293.
8 J. N. Cha, G. D. Stucky and D. E. Morse, *Nature*, 2000, **403**, 403–407.
9 H. Menzel, S. Horstmann, P. Behrens, P. Baernreuther, I. Krueger and M. Jahns, *Chem. Commun.*, 2003, **24**, 2994–2995.
10 S. V. Patwardhan, N. Mukherjee and S. J. Clarson, *Silicon Chem.*, 2002, **1**, 47–55.
11 G. M. Gratson and J. A. Lewis, *Langmuir*, 2005, **21**, 457–464.
12 D. B. Chrisey, *Science*, 2000, **289**, 879.
13 G. Pohnert, *Angew. Chem., Int. Ed.*, 2002, **41**, 3167–3169.
14 J. J. Harris, P. M. DeRose and M. L. Bruening, *J. Am. Chem. Soc.*, 1999, **121**, 1978–1979.
15 K. H. Sandhage, M. B. Dickerson, P. M. Huseman, M. A. Caranna, J. D. Clifton, T. A. Bull, T. J. Heibel, W. R. Overton and M. E. A. Schoenwaelder, *Adv. Mater.*, 2002, **14**, 429.
16 R. R. Unocic, F. M. Zalar, P. M. Sarosi, Y. Cai and K. H. Sandhage, *Chem. Commun.*, 2004, **7**, 796–797.
17 Y. A. Vlasov, X. Z. Bo, J. C. Sturm and D. J. Norris, *Nature*, 2001, **414**, 289–293.